

Compaction effects on strains within profiled thermoplastic pipes

R. W. I. Brachman¹, I. D. Moore² and S. M. Munro³

¹Associate Professor, GeoEngineering Centre at Queen's-RMC, Queen's University, Kingston, Canada, K7L 3N6, Telephone: +1 613 533 3096, Telefax: +1 613 533 2128, E-mail: brachman@civil.queensu.ca

²Professor and Canada Research Chair in Infrastructure Engineering, GeoEngineering Centre at Queen's-RMC, Queen's University, Kingston, Canada, K7L 3N6, Telephone: +1 613 533 3160, Telefax: +1 613 533 2128, E-mail: moore@civil.queensu.ca

³Project Engineer, Jacques Whitford, 3 Spectacle Lake Drive, Dartmouth, Canada, B3B 1W8, Telephone: +1 902 468 7777, Telefax: +1 902 4689009, E-mail: Scott.Munro@jacqueswhitford.com

Received 18 April 2007, revised 2 October 2007, accepted 2 October 2007

ABSTRACT: Results from laboratory tests are reported to establish how pipe deflections, strains and local bending are influenced by the selection of backfill soil and its placement for two profiled thermoplastic culverts. Lined-corrugated high-density polyethylene (HDPE) and polyvinyl chloride (PVC) pipes with a nominal inside diameter of 600 mm were tested in poorly graded sand and well-graded gravel backfills. The backfill was compacted using real compaction equipment and procedures, and then subjected to a maximum increase in vertical pressure of 200 kPa in a test cell that simulates deep burial. For the specific conditions tested, the largest deflections and strains were for the HDPE pipe when placed just above a rigid base and with uncompacted sand backfill placed below the springline, while local bending was greatest for the PVC pipe with well-compacted gravel backfill. A procedure is presented to account for the maximum local bending strain within a simplified design approach for profiled thermoplastic pipes using an empirical strain factor inferred from the measured results.

KEYWORDS: Geosynthetics, Geopipes, Profiled thermoplastic culverts, Local bending, Construction practice, Design

REFERENCE: Brachman, R. W. I., Moore, I. D. & Munro, S. M. (2008). Compaction effects on strains within profiled thermoplastic pipes. *Geosynthetics International*, 15, No. 2, 72–85. [doi: 10.1680/gein.2008.15.2.72]

1. INTRODUCTION

Thermoplastic (e.g. high-density polyethylene, HDPE; polyvinyl chloride, PVC) pipes for culverts and sewers often feature pipe walls with profiled geometry (as opposed to solid pipe walls). Figure 1 shows one such profile, featuring circumferential corrugations and an interior liner, referred to as a lined-corrugated pipe. Figure 1 also defines the terminology used to describe circumferential (θ) locations around the pipe (Figure 1a) and elements of the profile (Figure 1b).

The criteria (i.e. limit states) that need to be evaluated in the design for profiled thermoplastic pipes relate to pipe deflection, pipe strains, global pipe stability, and local profile stability. Pipe deflections are limited below allowable levels to maintain serviceability of the culvert and implicitly limit the pipe strains. Pipe strains are kept below maximum compressive and tensile values as ductile failure can arise from excessive compressive strains, and stress cracking may occur under sustained long-term

tensions. An advantage of limiting strain, rather than stress, is that strain can be directly measured, and accumulation of strain with time is relatively small (relative to changes in stress) because the pipe deflections are controlled by the soil, which has relatively small creep effects. The pipe profile must be sufficient to prevent local buckling of the slender elements of the profile (Dhar and Moore 2001).

The interaction between soil and pipe will ultimately control how the pipe behaves with respect to the performance limits for these types of pipe. The structural performance of thermoplastic pipes consequently depends on the stiffness of the pipe (influenced by its material properties, profile geometry, and diameter), and on the stiffness of the backfill soil surrounding the pipe (related to the type of soil, density, confining stress, and strain level). The backfill configuration (e.g. the type and extent of soil materials) and the method of compaction can also impact on the nature of loading and support for the pipe.

When buried and subject to earth pressures, these pipes

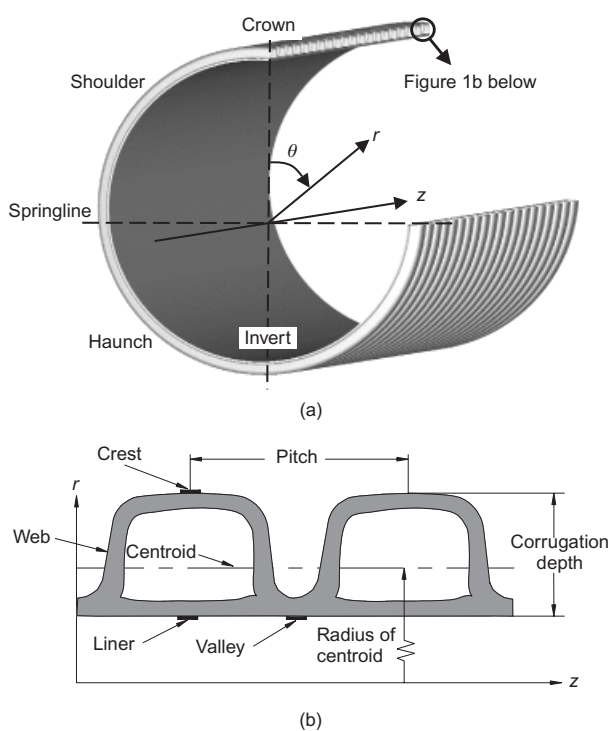


Figure 1. (a) Section through lined-corrugated pipe; (b) cross-section of pipe wall showing location of strain gauges at crest, valley and liner of the profile

experience deformations and strains arising both from circumferential compression and from bending. In addition to the bending that arises because the vertical earth pressures normally exceed the horizontal earth pressures, local bending may also occur from non-uniform soil loading and/or support around the pipe.

One cause of local bending is poor soil support under the haunches of the pipe (see Figure 1). Because it is difficult to place and compact backfill soil beneath the haunches, the soil in this region may be less dense and consequently have lower stiffness than at other locations around the pipe. This results in non-uniform support for

the pipe, and produces local bending. Non-uniform soil support, and hence local bending, can also result from the presence of stiff ground underlying the invert.

The extent of local bending may be expected to depend on the stiffness of the pipe and the nature of the non-uniform soil support (influenced by type of backfill, method of construction, extent of construction supervision, etc.). While Dhar *et al.* (2004) have numerically investigated the effects of an idealised soft haunch zone on the strains in profiled thermoplastic pipes, there is a paucity of measured data to quantify local bending effects in these structures.

The objectives of this paper are to examine the effects of backfill compaction on pipe deflections and strains, and quantify local bending effects in the pipe. Results from six experiments are reported where the pipe was backfilled and compacted using real compaction equipment and then subjected to increases in vertical and horizontal stresses corresponding to those expected under deep burial. Both HDPE and PVC lined-corrugated pipes with a nominal inside diameter of 600 mm were tested. Three different burial conditions and two backfill materials were tested to examine the effect of compaction on the overall pipe response and local bending. An approach to account for local bending effects within a simplified design procedure is proposed.

2. EXPERIMENTAL DETAILS

2.1. Test apparatus

The experiments were conducted using the laboratory test cell developed by Brachman *et al.* (2001). The test cell simulates the vertical and horizontal earth pressures associated with burial beneath an embankment, and permits examination of burial conditions, installation practices, and compaction techniques. The test cell is 2.0 m wide, 2.0 m long and 1.6 m high, and is capable of testing pipes of up to 700 mm in diameter. A cross-section through the test cell is shown in Figure 2.

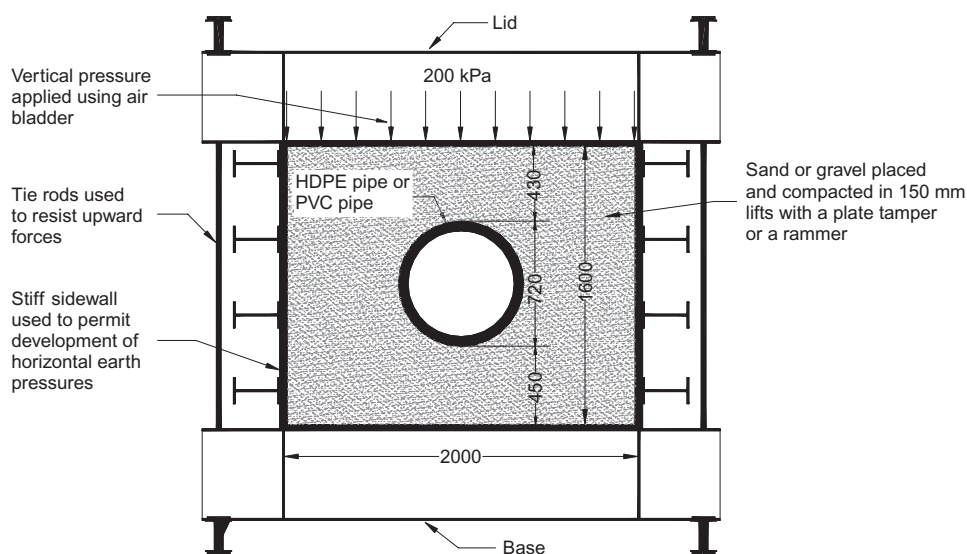


Figure 2. Cross-section through biaxial test cell showing backfill geometry for tests T1, T2, T5 and T6 (dimensions in mm)

Vertical pressures are applied to the ground surface using a pressurised air bladder. Horizontal stresses corresponding to conditions of zero lateral strain (i.e. K_0 conditions) are developed by limiting the lateral deflection of the test cell walls to negligible levels with stiff side-walls. The experiments reported in this paper were conducted to a maximum vertical pressure of 200 kPa (equivalent to the vertical stress imposed by the weight of a 10 m deep embankment with a unit weight of 20 kN/m³). The vertical pressure was applied in successive 25 kPa increments, with each increment held for 10 min to permit measurements to be taken after the soil and pipe responses had stabilised.

Friction between the walls and backfill soil was minimised by placing polyethylene sheets lubricated with high-temperature bearing grease along the walls. This arrangement reduces the boundary friction to less than 5° (Tognon *et al.* 1999), and leads to less than a 5% decrease in vertical stresses reaching the pipe (Brachman *et al.* 2001). The ends of the pipe were not restrained in the axial direction, to avoid interference from the walls of the test cell. A ring cut out of rigid foam board and placed at both ends of the pipe was used to prevent sand from falling into the gap between the ends of the pipe and the test cell (Munro 2006).

2.2. Materials

Two types of lined-corrugated thermoplastic pipe were used in this study, both having nominal internal diameters of 600 mm. An HDPE pipe was used in tests T1-T3 and T5, and a PVC pipe was used in T4 and T6. Profile geometries for both of these pipes are summarised in Table 1, with the relevant terminology defined in Figure 1b.

Table 1. Sectional properties of the HDPE and PVC lined-corrugated pipes tested

Property	HDPE pipe	PVC pipe
Internal diameter (mm)	603	592
Pitch (mm)	101	48
Corrugation depth, h (mm)	55.2	27.1
Radius to neutral axis, R (mm)	323	308
Area of pipe wall, A (mm ² /mm)	9.3	4.4
Moment of inertia of pipe wall, I (mm ⁴ /mm)	3104	6660

Two different backfill materials were used. The backfill material used in the first four tests was a poorly graded sand (synthetic olivine, with Unified soil classification SP) with a mean grain size of 0.5 mm, a uniformity coefficient C_u of 1.46, a curvature coefficient C_c of 0.94, and an angle of internal friction of 44° (Lapos and Moore 2002). Minimum and maximum dry densities are 1.31 g/cm³ and 1.55 g/cm³, respectively. For the fifth and sixth tests a well-graded gravel (Unified soil classification GW) was used. This gravel had a mean grain size of 5.5 mm, a uniformity coefficient C_u of 12.5, and a curvature coefficient C_c of 1.62. Minimum and maximum dry densities are 1.50 g/cm³ and 1.98 g/cm³, respectively.

2.3. Test conditions

The conditions for each test are summarised in Table 2. All tests were conducted at a temperature of 22 ± 2°C. For each of the tests, the densities were obtained as the test cell was backfilled using a nuclear density gauge, and these are reported in Figure 3.

In test T1, the sand was placed in 150 mm thick lifts that were compacted by two passes with a vibratory plate tamper (M-B-W AP2000S). The base of the plate tamper measured 48 cm × 53 cm. The resulting sand density was essentially uniform, with an average dry density of 1.49 g/cm³, corresponding to a density index I_D of 78%, and ranging between 1.47 and 1.51 g/cm³, as shown in Figure 3a. No additional effort was made to compact the soil in the pipe haunches. In test T2, the sand was also placed in 150 mm thick lifts, but each was compacted by two passes with a rammer (Wacker ES52Y). The rammer had a baseplate size of 25 cm × 33 cm, which enabled it to provide greater compaction in the haunch region relative to the plate tamper. The average dry density for T2 was 1.51 g/cm³ ($I_D = 86%$) with a range between 1.48 and 1.53 g/cm³, as shown in Figure 3b. This suggests that the rammer delivered higher compactive effort than the plate tamper, as it resulted in higher density measurements.

In tests T3 and T4 the pipe was placed just above a stiff base with uncompacted sand backfill below the springlines and denser backfill above the springline, as shown in Figure 4. Concrete blocks were first placed at the base of the test cell to simulate a hard foundation for the pipe. A 70 mm thick bedding of compacted sand was then placed over the hard surface, since it was considered unreasonable to expect the pipes to be subject to direct placement on the rigid base. The pipe was then positioned on the

Table 2. Summary of tests performed

Test	Description ^a	Backfill material	Type of pipe	Compaction
T1	SP-HDPE-PT	Sand	HDPE	Plate tamper
T2	SP-HDPE-R	Sand	HDPE	Rammer
T3	SP-HDPE-SB	Sand	HDPE	Stiff base with a loose haunch
T4	SP-PVC-SB	Sand	PVC	Stiff base with a loose haunch
T5	GW-HDPE-PT	Gravel	HDPE	Plate tamper
T6	GW-PVC-PT	Gravel	PVC	Plate tamper

^aSP, poorly graded sand; GW, well-graded gravel; HDPE, high-density polyethylene; PVC, polyvinyl chloride; PT, plate tamper; R, rammer; SB, stiff base/loose haunch.

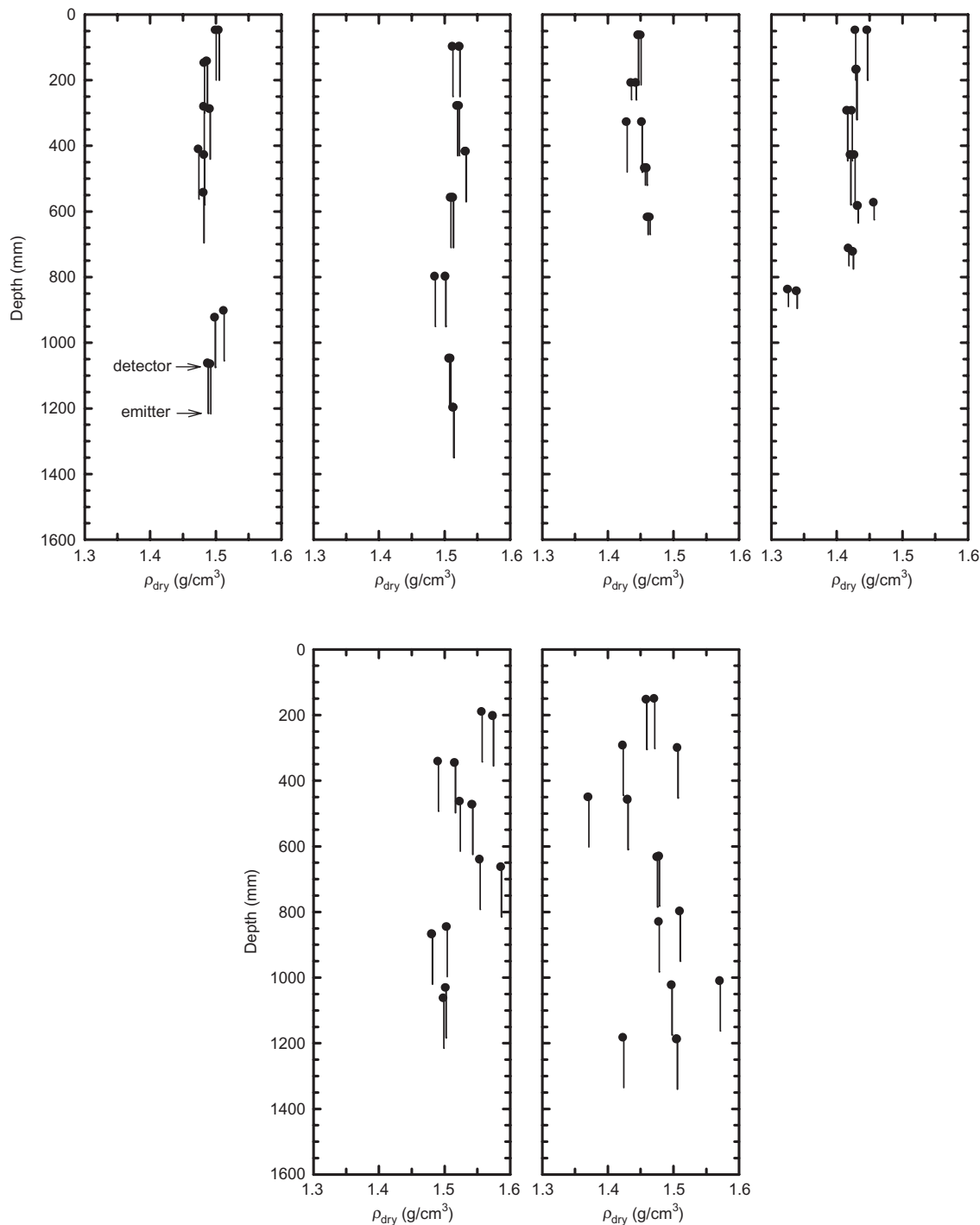


Figure 3. Local density measurements taken with depth for (a)–(d) pipes tested in a poorly graded sand and (e), (f) pipes tested in a well-graded gravel: (a) T1, SP-HDPE-PT; (b) T2, SP-HDPE-R; (c) T3, SP-HDPE-SB; (d) T4, SP-PVC-SB; (e) T5, GW-HDPE-PT; (f) T6, GW-PVC-PT

bedding material, and the sand was placed without compaction up to the level of the springlines, with no special efforts to place soil in the haunches. From the springline to the top of the test cell, the sand was placed in 150 mm thick lifts and manually compacted (two passes dropping a 250 mm square plate with 6.8 kg mass a distance of 0.4 to 0.5 m). The resulting densities in T3 and T4 (Figures 3c and 3d) were much lower than in T1 or T2. The overall dry density for T3 was 1.45 g/cm³ ($I_D = 62%$) above the springline and 1.35 g/cm³ ($I_D = 19%$)

below, while the dry density for T4 was 1.43 g/cm³ ($I_D = 54%$) above and 1.34 g/cm³ ($I_D = 14%$) below the springline.

Gravel backfill was used in tests T5 and T6. It was placed in 150 mm thick lifts, with each lift compacted by two passes of a vibratory plate tamper (Bomag BP 10/36-2). The Bomag vibratory plate tamper had a baseplate size of 56 cm × 36 cm. The densities obtained with the gravel (Figures 3e and 3f) were greater than those for the sand, as expected for a well-graded material. The average

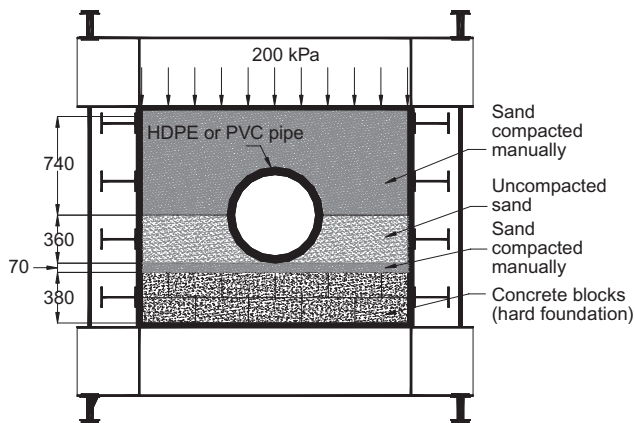


Figure 4. Cross-section through biaxial test cell showing backfill geometry of tests T3 and T4 (dimensions in mm)

of all dry densities for T5 was 1.83 g/cm^3 ($I_D = 74\%$), with values ranging from 1.79 to 1.89 g/cm^3 . The average dry density obtained for T6 was 1.77 g/cm^3 ($I_D = 63\%$), with values ranging from 1.67 to 1.87 g/cm^3 . The greater scatter in density reading with gravel is attributed to the presence of larger-size particles than in the sand.

2.4. Strain gauges

Surface strains of the pipe were measured using electrical resistance foil gauges with a 2 mm gauge length (Showa N22-FA-2-120-11, accurate to within $\pm 10 \mu\epsilon$). Up to 30 biaxial gauges were used to measure pipe wall strains in both the circumferential (ϵ_θ) and axial (ϵ_z) directions. A close spacing of measurements in one of the lower haunches (between $\theta = 90^\circ$ and 180°) was chosen to detect any local bending effects in that zone.

Strains measured on the HDPE pipe were adjusted for local gauge stiffening (since the stiffness of the strain gauge and adhesive is similar to that of the pipe) by multiplying each strain reading by a factor unique to that gauge, ranging from 1.13 to 1.45. These were obtained by dividing the strain computed from deflection measurements (i.e. independent of the strain gauges) by measurements with the strain gauges, during an unrestrained thermal contraction test from 22°C to 0°C (specific details are reported by Munro 2006). No adjustment of strain measurements was applied for the PVC pipe given its higher modulus relative to the gauges. Compressive strains are reported as negative values. The strain readings were zeroed after backfilling was complete.

3. RESULTS

3.1. Pipe deflection

Measured changes in vertical (ΔD_v) and horizontal (ΔD_h) diameter are shown in Figures 5 to 7 and are summarised in Table 3 at an applied pressure of 200 kPa. These values were measured using linear potentiometers mounted across the vertical and horizontal diameters to an accuracy of $\pm 0.01 \text{ mm}$. Increases in diameter are represented as positive values. All readings were zeroed prior to the application of vertical pressure.

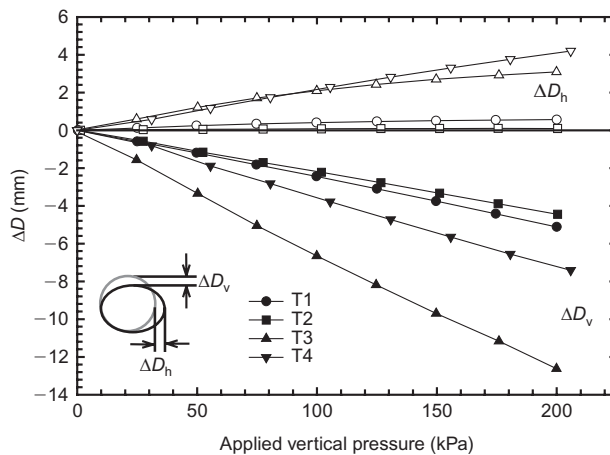


Figure 5. Measured vertical and horizontal diameter changes for T1–T4

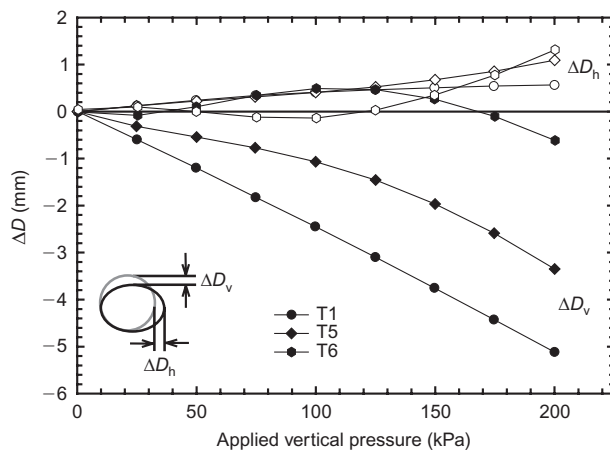


Figure 6. Measured vertical and horizontal diameter changes for T1, T5 and T6

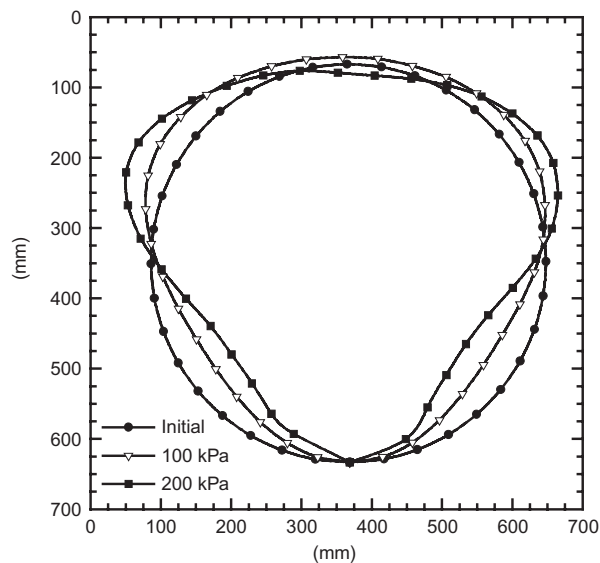


Figure 7. Deformed shape of pipe in T6 ($\times 20$ magnification)

Table 3. Vertical and horizontal deflections at 200 kPa

Test	Description	ΔD_v (mm)	ΔD_h (mm)	$\Delta D_v/\Delta D_h$
T1	SP-HDPE-PT	-5.1	0.6	-9
T2	SP-HDPE-R	-4.5	0.1	-44
T3	SP-HDPE-SB	-12.6	3.1	-4
T4	SP-PVC-SB	-7.4	4.2	-2
T5	GW-HDPE-PT	-3.4	1.1	-3
T6	GW-PVC-PT	-0.6	1.3	-1

Figure 5 shows the influence of three different burial conditions on HDPE pipe deflections when buried in the poorly graded sand. The decrease in vertical diameter was essentially linearly proportional to the applied overburden over the pressure range tested for T1 and T2. The vertical diameter change from T2 was 15% smaller than that from T1 (at 200 kPa), indicating that the slightly higher density obtained with the rammer led to a higher soil stiffness, resulting in smaller pipe deflection. When tested with the stiff base beneath the pipe and uncompacted sand below the springlines in T3, the vertical deflections of the HDPE pipe are 2.8 times larger than those for T1. There also appears to be some stiffening of the initially uncompacted sand in T3, as indicated by the decreasing rate of diameter change beyond 100 kPa.

To place all of these measured values in context, the allowable deflection for such a profiled wall HDPE pipe is normally limited to 7.5% of the inside pipe diameter (ASTM F894). The measured maximum vertical diameter changes correspond to 0.85%, 0.74% and 2.1% of the inside pipe diameter for T1, T2 and T3, respectively, and are much smaller than the 7.5% deflection limit.

Burial condition also has an influence on the horizontal deflections plotted in Figure 5. The smallest horizontal deflections were measured in T2, where the soil density was highest. In both T1 and T2 the increase in the horizontal diameter is small relative to the decrease in vertical diameter. While this may be attributed partially to resistance to outward horizontal pipe movement from the stiff soil (e.g. Moser 2001), it can be demonstrated (using the Fourier decomposition employed in the Hoeg (1968) solution, e.g. Moore 2001) that stiff backfill leads to much higher levels of circumferential shortening, so that the uniform component of inward movement of the pipe counteracts most of the outward movements at the springline associated with the ovaling component of deflection. With the more complex backfill support conditions in T3, the ratio of horizontal to vertical diameter change is larger than for T1 or T2. This suggests that, in addition to circumferential shortening experienced in T3, there are some effects from the uncompacted sand below the springline. The deformed shape is different in T3 relative to T1 and T2, and this produces greater bending strains, as examined later.

The results in Figure 5 also show the differences in pipe deflection between the HDPE and PVC pipes when tested with the rigid base beneath the pipe and uncompacted sand below the springline (T3 compared with T4). The vertical deflection of the HDPE pipe is 1.7 times greater

than that for the PVC pipe. As expected for the same initial backfill condition, larger vertical deflections are obtained for the pipe with lower modulus. The role of circumferential pipe compression on deformed shape is further illustrated in that the horizontal deflection of the PVC pipe is slightly larger than that for the HDPE pipe. Here, the stiffer PVC pipe experiences less circumferential shortening relative to the more compressible HDPE pipe, resulting in horizontal deflection that is larger as a proportion of the vertical deflection.

Deflections for the HDPE pipe when backfilled with sand (T1) and gravel (T5) and plate tamper compaction are shown in Figure 6. As expected, the gravel resulted in smaller vertical deflection, since it is stiffer than the sand.

Vertical and horizontal diameter changes for the PVC pipe in gravel with plate tamper compaction (T6) are also shown in Figure 6. They are smaller than for the HDPE pipe in T5; however, the trend from this test differs from all others, showing an interesting response where there was an initial increase in vertical diameter to 125 kPa, followed by an overall decrease in vertical diameter. Fortunately, an additional technique for monitoring pipe deflections was employed for Test T6 that was used to corroborate and explain the measurements obtained with the linear potentiometers. This involved analysis of high-resolution digital photographs of the pipe shape using particle image velocimetry (White *et al.* 2003). The advantage of this technique is that the deformations around the entire circumference of the pipe are obtained. The accuracy of this technique was ± 0.025 mm.

The deformed shape of the PVC pipe from T6 is plotted in Figure 7. Since deflections in this test are small, the deformed shape has been exaggerated by a factor of 20 to illustrate the deformation pattern. This exaggerated deflection pattern should not be interpreted as global buckling. This pipe (with high flexural rigidity) in this high modulus soil has a very high factor of safety against global buckling at these simulated burial depths (see Moore 2001). Figure 7 shows that the deformed shape is not elliptical, but rather the shoulders deform outwards and the haunches move inwards (the 'heart shaped' deformation pattern identified by Rogers 1988). A slight increase in vertical diameter at 100 kPa and decrease in vertical diameter at 200 kPa can be seen, which is consistent with the measurements in Figure 6. Although the maximum decrease in vertical diameter was -0.6 mm, the overall maximum decrease in pipe diameter occurs between the shoulder and haunch along the diameter from 40° to 120° with a magnitude of -2.0 mm. The maximum increase in

pipe diameter still occurred across the springlines (i.e. at 90–270°). While the deformed shape in Figure 7 is interesting, and useful in understanding the resulting pattern of strains, the overall pipe deflections for T6 are small, as expected, and are well below the allowable diameter change of 6–7.5% (ASTM F949-06).

3.2. Pipe strain

3.2.1. Detailed results for T1

Circumferential strains, ε_θ , measured at the corrugation valley and crest are plotted against the applied pressure in Figure 8. As observed for pipe deflections, the measured strains show a nearly linear response with applied pressure. The maximum compressive strain occurred at the valley springlines ($\theta = 90^\circ$ and 270°), while the minimum was recorded at the crest invert.

Axial strains, ε_z , are presented in Figure 9. All values are tensile, except for the value at the exterior invert ($\theta = 180^\circ$). While both ε_θ and ε_z are required for any calculations of the resulting circumferential and axial stress, only values of ε_θ are reported for the remainder of this paper, since they are the major principal strains and are sufficient to quantify the backfill effects being studied, and their

influence on pipe response. Detailed reporting of all measured axial strains can be found in Munro (2006).

The distribution of ε_θ around the circumference of the pipe at 200 kPa is plotted in Figure 10. These results show that the strains at the liner were much less than at the valley. This arises from local bending effects in the profile (Moore and Hu 1996). Dhar and Moore (2002) demonstrated that the structural resultants (thrust and moment) for such profiled pipes should be quantified using the valley (interior) and crest (exterior) strains, even though they are not directly across from each other on the profile. Consequently, liner strains are reported only for T1; values for the other tests are presented by Munro (2006).

The circumferential bending experienced by the pipe can be assessed by comparing the relative magnitude of these crest and valley strains at a particular circumferential location (i.e. the average of the crest and valley strains can be attributed to circumferential thrust; the average of their difference is from circumferential bending). Figure 10 shows that at the crown, there was greater compression at the crest; at the springlines, the compression was greater at the valley; and at the invert, the compression was also greater at the valley. If the backfill around the pipe had uniform stiffness, no local soft zones, nor compaction-induced locked-in stresses (i.e. as assumed in the solution of Hoeg 1968), then it would be expected to have greater compression at the crest for both the crown and invert, and greater compression at the valley for the springlines. The measured results at the invert differ from uniform backfill, demonstrating additional local bending at or near the invert arising from the installation conditions. Modifications to uniform backfill calculations intended to account for such local bending effects are presented later in this paper.

There was no evidence of local instability of the profile elements, which is consistent with the small measured strains.

3.2.2. Influence of backfill condition

Figures 11 to 14 plot measured values of crest and valley strain at 200 kPa for the different conditions examined. The maximum compressive strain from each test is summarised in Table 4. In T1 to T5, the maximum strain was measured at (or very near) the springline in the profile valley. The maximum strain from T6 was located at the valley invert, suggesting that local bending near the invert has a substantial impact in that test. All measured strains are below the maximum allowable strains for the HDPE and PVC pipes (e.g. a 5% strain limit is specified in AASHTO M294-06).

Strain distributions for the HDPE pipe when buried in sand are shown in Figure 11. Since the rammer compaction produced denser sand backfill than the plate tamper, the strains for T2 are slightly smaller than those for T1. Local bending effects in the haunch are also greater in T1 than in T2. This is attributed to a softer haunch region in T1, which is likely since the vibrating plate compactor is less effective than the rammer at compacting the soil under the haunches.

Consistent with the deformation measurements, the

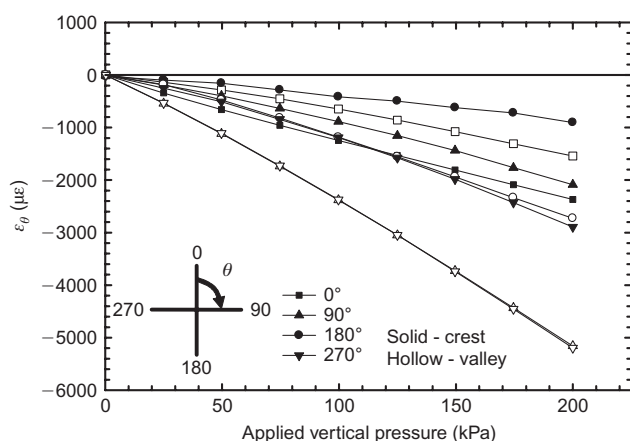


Figure 8. Circumferential strains at crown, invert and springlines for T1

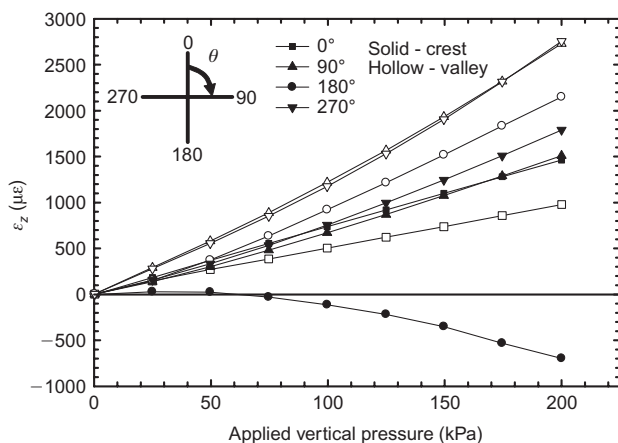


Figure 9. Axial strains at crown, invert, and springlines for T1

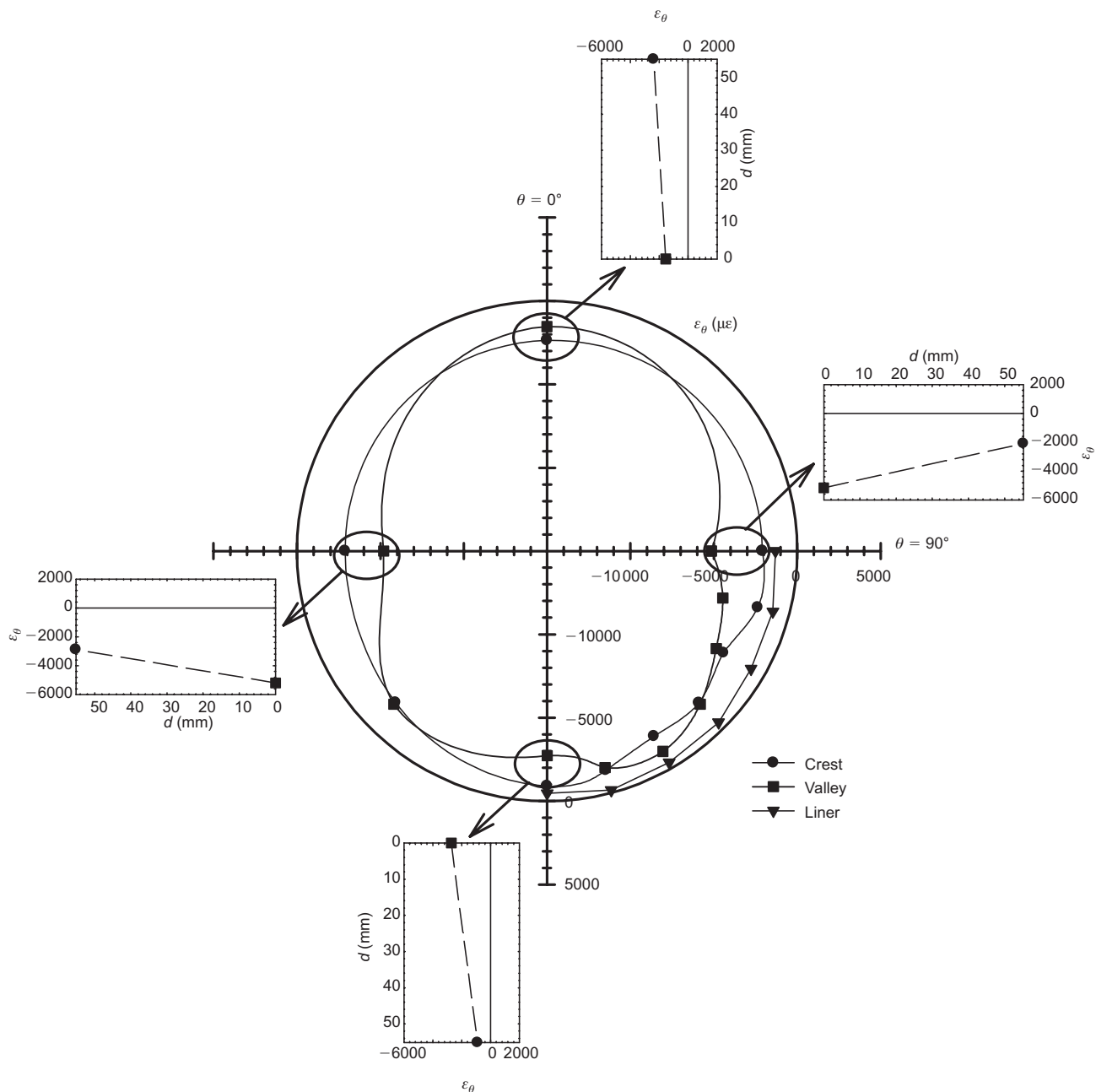


Figure 10. Distribution of circumferential strains at 200 kPa for T1 (d is the distance from the interior of the corrugation)

strains from T3 with a stiff base and uncompacted sand below the springlines are much larger than for T1 or T2, as shown in Figure 11. However, T3 does not appear to feature local haunch bending to the same extent as T1 or T2. While the soil in the haunch was placed uncompacted, it was placed in a consistent manner beneath the springline, providing essentially uniform, albeit poor, support to the pipe below the springlines. Consequently, no substantial local bending effects were observed in the vicinity of the haunches during T3. For the same reason, only small local bending effects were measured for the PVC pipe (T4) with the same stiff base soil and the same loose soil placed below the springlines (Figure 12).

The strains for the HDPE pipe with sand (T1) and gravel (T5) backfill and plate tamper compaction are compared in Figure 13. The maximum compressive strain

in T1 is slightly greater than that for T5, which is consistent with the gravel being stiffer than the sand. However, there are greater effects from local bending in T5, which result in tensile strains at the crest invert and valley haunch regions. That there is more local bending with the gravel is attributed to a greater discrepancy in stiffness between the soil below the haunch and the well-compacted zone away from the haunch. The PVC pipe, when tested with gravel backfill, showed a similar pattern of strain around the pipe (Figure 14), and even greater tensile strains from local bending. Although the tensile strains in Figure 14 are well below typical strain limits (e.g. AASHTO M294), these results indicate that these pipes buried in a stiff backfill are more susceptible to the effects of local bending, and that backfill conditions can lead to strains that deviate from those calculated from a uniform backfill analysis.

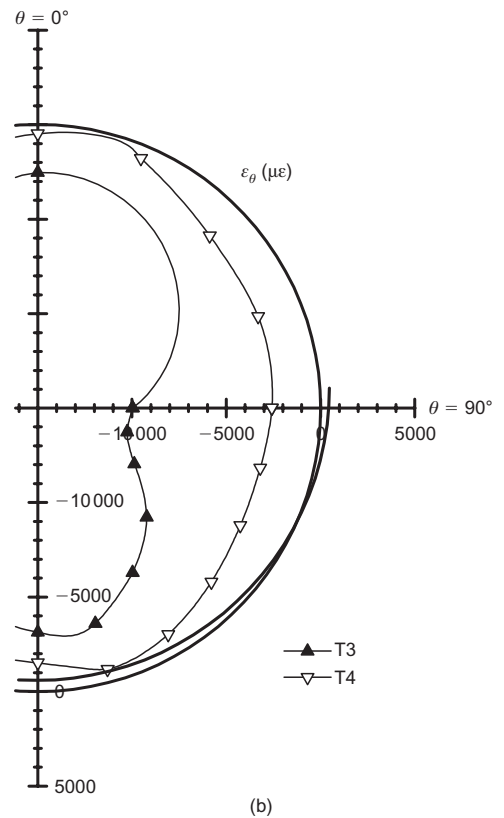
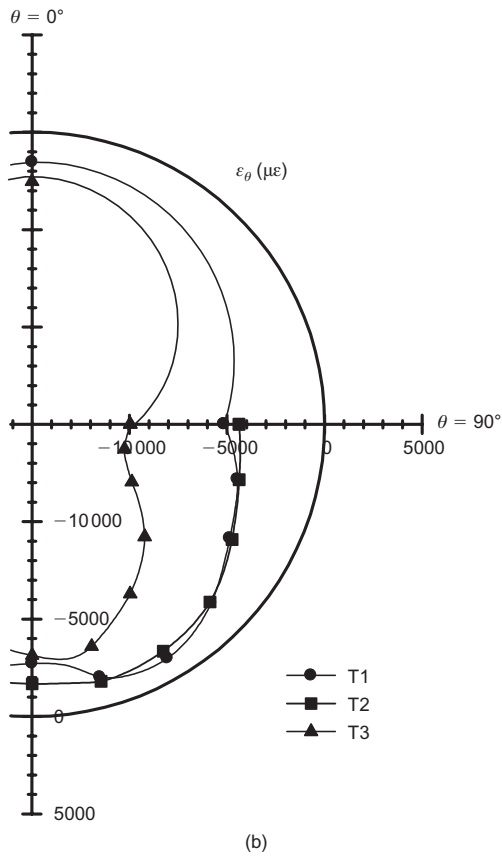
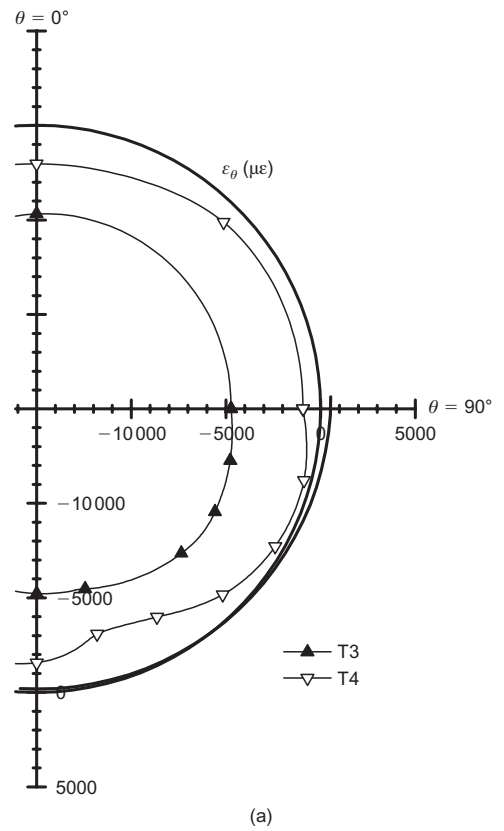
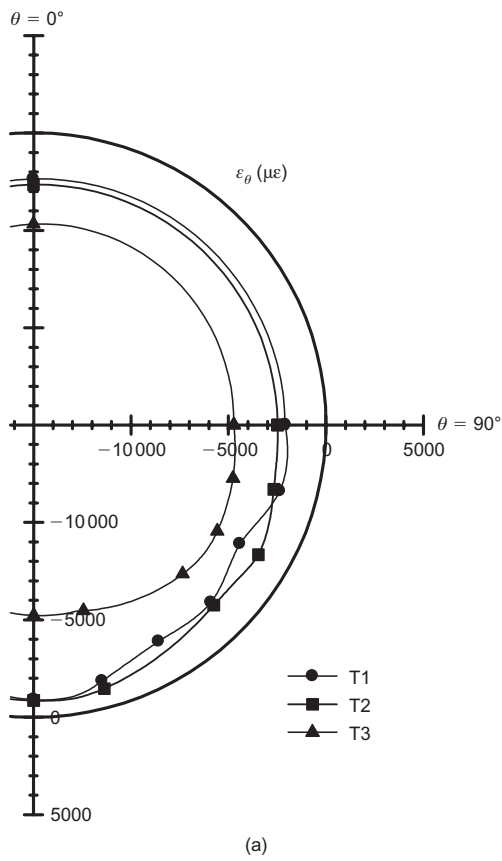
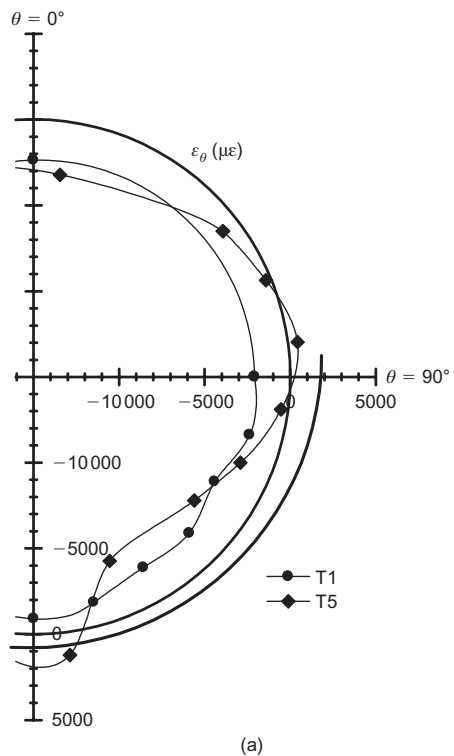
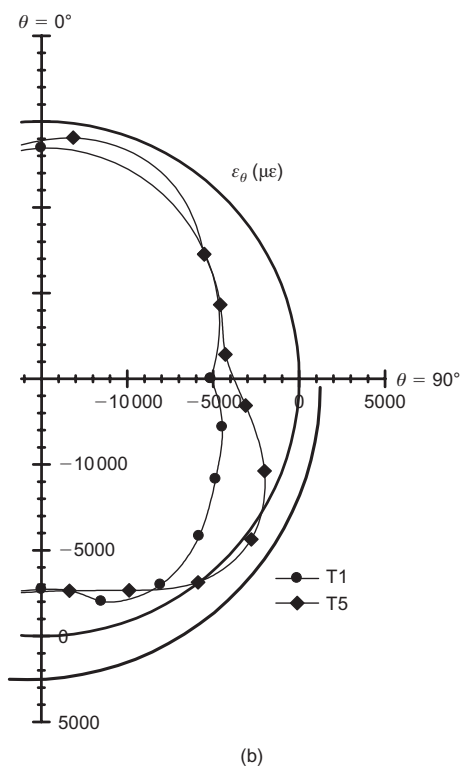


Figure 11. (a) Crest and (b) valley circumferential strains at 200 kPa for T1, T2 and T3

Figure 12. (a) Crest and (b) valley circumferential strains at 200 kPa for T3 and T4

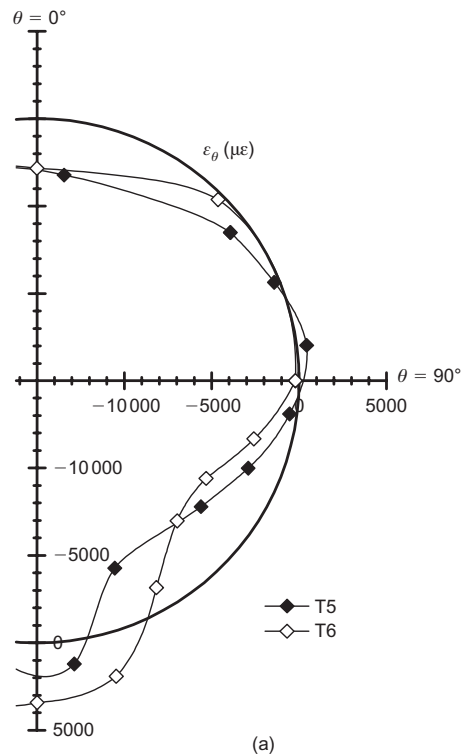


(a)

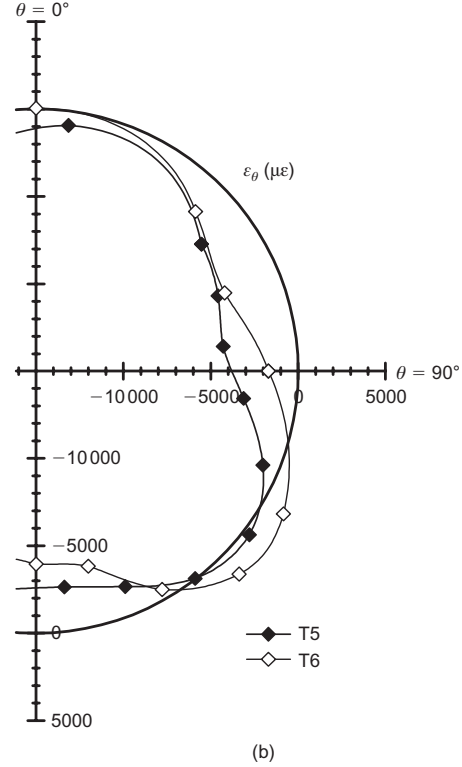


(b)

Figure 13. (a) Crest and (b) valley circumferential strains at 200 kPa for T1 and T5



(a)



(b)

Figure 14. (a) Crest and (b) valley circumferential strains at 200 kPa for T5 and T6

4. DISCUSSION

4.1. Accounting for local bending in design

There are several methods that can be used to obtain estimates of pipe deflections and strains for pipe design. For higher-risk projects (e.g. where the pipe loading and/or support may not be well defined, and/or the consequences of failure are high), non-linear finite element

analysis (e.g. Dhar *et al.* 2004) and laboratory testing (like that reported in this paper) may be required. However, for most conventional culvert applications, pipe deflections and strains can be calculated using design equations.

McGrath (1998) proposed a simplified design procedure specifically for flexible thermoplastic pipes. Vertical diameter decrease is obtained considering deflection resulting from both hoop compression and bending. In this proce-

Table 4. Measured maximum compressive circumferential strains located on the valley profile at 200 kPa

Test	Description	$\varepsilon_{\theta_{\max}}$ ($\mu\varepsilon$)	θ°
T1	SP-HDPE-PT	-5 200	-90
T2	SP-HDPE-R	-4 460	-90
T3	SP-HDPE-SB	-10 350	-90
T4	SP-PVC-SB	-2 880	-90
T5	GW-HDPE-PT	-4 350	-83
T6	GW-PVC-PT	-3 960	180

where, the peak circumferential bending strain ε_b is related to the bending component of deflection via

$$\varepsilon_b = D_f \left(\frac{c}{R} \right) \left(\frac{\Delta_b}{D} \right) \quad (1)$$

where c is the distance to the extreme fibre from the neutral axis of the pipe wall, R is the radius to the neutral axis of the pipe wall, D is the pipe diameter measured to the neutral axis of the pipe wall, Δ_b is the component of diameter change from bending, and D_f is an empirical strain factor relating the bending strain to bending deflection.

Since the magnitude of bending strain varies around the pipe circumference, it is useful to calculate local (rather than maximum) values of D_f using those local bending strains. The pattern of local D_f values around the circumference reflects the nature of local bending. For reference, an incompressible pipe subject to pure bending has a maximum value of $D_f = 3$, where maximum bending strains develop at the crown, springlines and invert. For this reference case, the local values of D_f are equal to zero at the shoulders and haunches.

The strain results presented in the previous section are now used to calculate patterns of local D_f values, and the manner in which they change with backfill condition in the six tests that were conducted. Expressing the bending strain in the pipe as the difference between the circumferential strains measured at the crest and valley ($\varepsilon_{\text{crest}}$ and $\varepsilon_{\text{valley}}$, respectively) and taking the bending deflection as one-half of the difference between measured values of

vertical (ΔD_v) and horizontal (ΔD_h) diameter change, local strain factor D_f was calculated using

$$D_f = \left(\frac{D^2}{h} \right) \left(\frac{\varepsilon_{\text{crest}} - \varepsilon_{\text{valley}}}{\Delta D_v - \Delta D_h} \right) \quad (2)$$

where h is equal to the corrugation depth, and the results are summarised in Table 5 for various locations around the pipe at 200 kPa. Negative values indicate that the radius of curvature of the pipe has decreased; the absolute value should be used in design. Deviations in local strain factor at the crown, springlines and invert relative to the reference case discussed above (where $D_f = 3$) can be attributed to local bending associated with backfill conditions. The two items of interest here are

- the magnitude and location of the maximum value of D_f in each test, which shows where local bending effects are greatest; and
- the magnitude of D_f required to calculate the overall maximum circumferential bending strain using the simplified design Equation 1.

The maximum strain factor obtained in T1 was observed to be 4.1, located at the springline of the pipe. Since this value is greater than 3, it implies that local bending induced by the soft haunch results in increases in bending strain at the springline, as previously discussed in reference to Figure 11. That the rammer compaction in T2 resulted in greater haunch support and less local bending than T1 is consistent with the maximum D_f of 3.2 located at the springlines for T2. Since the maximum values of D_f occur at the springline for both T1 and T2, these values would be required to obtain the maximum strain using Equation 1.

Dhar *et al.* (2004) reported measured deflections and strains for the same type of HDPE pipe as in T1, using the same test cell, but with a different sand that was hand-tamped to 85% of its standard Proctor maximum dry density (T1 was compacted to 98% of its standard Proctor maximum). Using Equation 2, $D_f = 2.6$ was calculated at the springline at 200 kPa from the results measured by Dhar *et al.* (2004). This suggests that more effective compaction of the backfill in T1 (relative to Dhar *et al.*

Table 5. Empirical strain factors, D_f , at 200 kPa

Test	Description	Crown	Springlines		Invert	Haunch	
		0°	90°	270°	180°	D_f	θ°
T1	SP-HDPE-PT	1.1	-4.1	-3.1	-2.4	-2.9	105
T2	SP-HDPE-R	-	-3.2	-2.7	-1.4	-2.9	105
T3	SP-HDPE-SB	1.0	-2.5	-2.2	1.0	-2.7	105
T4	SP-PVC-SB	1.9	-2.0	-2.4	-	-2.9	105
T5	GW-HDPE-PT ^a	3.9	-8.1	-7.2	-6.6	-6.1	128
T6	GW-PVC-PT	13	-6.7	-9.3	-33	-25	165

^aThe pipe specimen rotated 8° during installation of T5, so values were obtained at $\theta = 8^\circ, 83^\circ, 278^\circ$ and 172° .

2004, but both with no special efforts to compact the soil under the haunches) results in greater local bending. This is most likely from greater discrepancy in density between the haunch region and that away from the pipe when the soil experiences greater compactive effort. Although local bending is larger in the test with greater compaction (T1), the overall deflections and strains are much smaller with the greater compaction. The clear benefit of greater soil compaction is demonstrated by a vertical diameter decrease that was 5.5 times larger and circumferential strain at the valley springline that was 3.5 times larger in the test reported by Dhar *et al.* (2004), compared with T1.

The results in Table 5 for both T3 and T4 show maximum D_f values of just less than 3 occurring in the haunch region. Slightly lower D_f values were calculated at the springlines, where the maximum strains were recorded. Although the stiff base and uncompacted sand beneath springlines did result in overall large deflections and strains, they were not greatly enhanced by local bending effects. Consequently, a value of $D_f = 3$ would conservatively capture the maximum bending strain at the springline for this particular backfill configuration.

The value of D_f required to capture the maximum bending strain (located just above the springline) in T5 is -8.1 , as shown in Table 5 for 200 kPa. This is much larger than the value for T1, which is reflective of the greater local bending in T5 compared with T1. The overall maximum D_f in T5 was -9.3 (also just above the springline), but this was not observed at 200 kPa; it actually occurred at a lower pressure of 100 kPa. This can be explained by the change in slope of the diameter change plot beyond 100 kPa, as previously noted in reference to Figure 6, which leads to slightly larger local bending at a lower pressure.

When D_f was calculated for T6 using the measured deflections, unrealistically high values were obtained as a result of very small bending deflections caused by the measured changes in vertical and horizontal deflections (Figure 6). Consequently the values reported in Table 5 for T6 were obtained with calculated values of bending deflections using the design approach of McGrath (1998):

$$\frac{\Delta_b}{D} = \frac{D_1 K q_v}{(EI/R^3) + 0.061 M_s} \quad (3)$$

where q_v is the vertical soil pressure (200 kPa), E is the modulus of the pipe (2760 MPa), I is the moment of inertia of the pipe (6660 mm⁴/mm), R is the radius to the neutral axis of the pipe wall, D_1 is a deflection lag factor (equal to 1 for this test condition), K is a bedding coefficient (equal to 0.083, corresponding to 180° bedding) and M_s is the constrained soil modulus (96 MPa); the values used for T6 are given in parentheses. The resulting D_f values for T6 are still much larger than for the other tests. A D_f value of 33 would be required to obtain the maximum bending strain observed in this test at the invert. The large D_f values can be attributed to high differences in bending strains coupled with small deflections as a result of high stiffness backfill, along with the fact that PVC has a higher pipe modulus than that of HDPE.

4.2. Implications for pipe design

The results in Table 5 show that strain factor is influenced by the burial condition, the type of pipe, and the backfill material. The final choice of strain factor for use in design should be made considering what combinations of soil stiffness and deflection are capable of bringing the pipe to its performance limits (assuming a contractor is permitted to bury the pipe and induce, say, 5% decrease in vertical pipe diameter). The tests reported here demonstrate that it is unnecessarily conservative to use pipe deflections of 5% in strain calculations, where those large deflections are employed together with a high strain factor that is achieved only when using well-compacted, well-graded backfills that feature a restricted zone of loose backfill. While the final values adopted for use in design standards are based on committee discussions that bring input from a variety of sources, the results presented here indicate that a maximum D_f value no greater than 5 is reasonable for conventional installations (those under 10 m deep burial) featuring maximum pipe deflections (decrease in vertical diameter) of say 5%. Higher values of D_f would need to be used, however, where the pipe is placed under deep burial and highly compacted backfill is used to enhance backfill stiffness to control pipe deformations.

5. CONCLUSIONS

Results were reported from six experiments conducted to examine the influence of soil material and backfill compaction on the deflections and strains of lined-corrugated HDPE and PVC pipes. A procedure has been presented to account for the maximum local bending strain within a simplified design approach for profiled thermoplastic pipes, based on an empirical strain factor D_f inferred from the measured results.

For the particular conditions examined, the largest deflections were for the HDPE pipe when placed just above a rigid base and with uncompacted sand backfill placed below the springline. The circumferential strains were also largest in this test, with the maximum values measured at the profile valley at the springline. Although the strains were large, they were not greatly affected by local bending in the haunch, as the backfill sand provided essentially uniform, albeit poor support. Use of a strain factor $D_f = 3$ would conservatively capture the maximum bending strain for this configuration.

For the tests on the HDPE pipe with compacted sand backfill (hand tamped, plate tamper and rammer compaction, all with no special efforts to compact beneath the haunches) the deflections and strains were slightly smaller with the rammer than the plate tamper, and both were much smaller than when hand tamped. Of these three tests, local bending was most prominent for construction with the plate tamper. This was attributed to a greater difference in density between the haunch and the surrounding soil, leading to less uniform soil support. Local bending was less with the rammer because it was more effective at compacting the soil placed under the pipe haunches. A strain factor of $D_f = 4$ for the test with the

plate tamper, and $D_f = 3$ for rammer and hand-tamped compaction, would be suitable to capture the peak bending strains in these particular configurations.

When the HPDE pipe was tested with stiff gravel backfill and plate tamper compaction (and no special effort to compact under the pipe haunches), the resulting pipe deflections and strains were smaller than for sand backfill; however, local bending effects were greater. This was attributed to even greater discrepancy in density between the poorly compacted haunch and the denser (and stiffer) soil at other locations around the pipe. Local bending was more prominent with the stiff gravel backfill than for sand, requiring $D_f = 9$ to capture the peak bending strain. The test with the PVC pipe and stiff gravel backfill also experienced small deflections and strains, but large local bending effects, with $D_f = 33$ required to capture the peak bending strain.

In six tests conducted, all measured short-term pipe deflections and strains were below allowable levels. The specific values of deflection, strain and strain factor reported in this paper are those for the particular pipe, backfill materials, backfill configuration, and compaction methods that were tested. They should not be directly applied for different conditions without careful evaluation, and are provided for consideration along with other pertinent factors by code committees and others charged with the responsibility of setting design requirements.

ACKNOWLEDGEMENTS

The research work was conducted as a part of NCHRP Project 4-26. Any opinions, findings, conclusions or recommendations expressed in this paper are those of the authors and do not necessarily reflect the views of the sponsors. The work was aided by valuable discussions with T. J. McGrath of Simpson, Gumpertz and Heger. The efforts of W. A. Take to obtain the deformed shape of the PVC pipe using his particle image velocimetry technique are greatly appreciated. Pipe specimens were donated by Contech Construction Products and Hancor Incorporated. The research equipment was funded in part by the Natural Sciences and Engineering Research Council of Canada and the Canada Foundation for Innovation.

NOTATIONS

Basic SI units are given in parentheses.

A	area of pipe wall (m^2/m)
c	distance to extreme fibre from neutral axis of pipe wall (m)
C_c	uniformity coefficient (dimensionless)
C_u	curvature coefficient (dimensionless)
D	pipe diameter measured to neutral axis of pipe wall (m)
d	radial distance from the interior of the corrugation (m)
ΔD	diameter change of pipe (m)
ΔD_v	vertical diameter change of pipe (m)
ΔD_h	horizontal diameter change of pipe (m)

D_f	empirical strain factor relating bending strain to bending deflection (dimensionless)
D_l	deflection lag factor (dimensionless)
E	Young's modulus of pipe (Pa)
h	corrugation depth (m)
I	moment of inertia of pipe (m^4/m)
I_D	density index (dimensionless)
K	bedding coefficient (dimensionless)
K_0	coefficient of lateral earth pressures for zero lateral strain (dimensionless)
M_s	constrained soil modulus (Pa)
R	radius to neutral axis of pipe wall (m)
r	radial coordinate (m)
q_v	vertical soil pressure (Pa)
z	axial coordinate (m)
Δ_b	component of diameter change from bending (m)
ε_θ	circumferential strain (dimensionless)
$\varepsilon_{\theta\text{max}}$	maximum circumferential strain (dimensionless)
ε_b	circumferential bending strain (dimensionless)
$\varepsilon_{\text{crest}}$	circumferential strains measured at crest of profile (dimensionless)
$\varepsilon_{\text{valley}}$	circumferential strains measured at valley of profile (dimensionless)
ε_z	axial strain (dimensionless)
θ	circumferential coordinate (degrees)
ρ_{dry}	dry density of soil (kg/m^3)

REFERENCES

- AASHTO M294-06. *Standard Specification for Corrugated Polyethylene Pipe, 300- to 1500-mm Diameter*, American Association of State Highway and Transportation Officials, 444 North Capitol Street NW, Suite 249, Washington, DC 20001.
- ASTM F894-07. *Standard Specification for Polyethylene (PE) Large Diameter Profile Wall Sewer and Drain Pipe*, ASTM International, West Conshohocken, PA, USA.
- ASTM F949-06. *Standard Specification for Poly(Vinyl Chloride) (PVC) Corrugated Sewer Pipe With a Smooth Interior and Fittings*, ASTM International, West Conshohocken, PA, USA.
- Brachman, R. W. I., Moore, I. D. & Rowe, R. K. (2001). The performance of a laboratory facility for evaluating the structural response of small-diameter buried pipes. *Canadian Geotechnical Journal*, **38**, No. 2, 260–275.
- Dhar, A. S. & Moore, I. D. (2001). Liner buckling in profiled polyethylene pipes. *Geosynthetics International*, **8**, No. 4, 303–326.
- Dhar, A. S. & Moore, I. D. (2002). Corrugated high density polyethylene pipe: Laboratory evaluation of two-dimensional analyses for limit states design. *Transportation Research Record: Journal of the Transportation Research Board*, No. 1814, 157–163.
- Dhar, A. S., Moore, I. D. & McGrath, T. J. (2004). Two-dimensional analysis of thermoplastic culvert deformations and strains. *Journal of Geotechnical and Geoenvironmental Engineering*, **130**, No. 2, 199–208.
- Hoeg, K. (1968). Stresses against underground structural cylinders. *Journal of Soil Mechanics and Foundation Engineering*, **94**, No. 4, 833–858.
- Lapos, B. & Moore, I. D. (2002). Evaluation of the strength and deformation properties of olimag synthetic olivine. *Proceedings of the 55th Canadian Geotechnical Conference*, Niagara Falls, pp. 729–734.
- McGrath, T. J. (1998). *Design Method for Flexible Pipe. A Report to the AASHTO Flexible Culvert Liaison Committee*, Simpson Gumpertz & Heger Inc., Arlington, MA.
- Moore, I. D. (2001). Buried pipes and culverts. *Geotechnical and Geoenvironmental Engineering Handbook*, Rowe, R. K., Editor, Kluwer Academic Publishing, Norwell, USA, 541–567.

- Moore, I. D. & Hu, F. (1996). Linear viscoelastic modelling of profiled high density polyethylene pipe. *Canadian Journal of Civil Engineering*, **23**, No. 2, 395–407.
- Moser, A. (2001). *Buried Pipe Design*, McGraw-Hill, New York.
- Munro, S. M. (2006). *Measurement of Backfill Effects on Circumferential Bending in Lined-Corrugated Thermoplastic Pipes and Fibre Reinforced Cement Pipes*. MSc thesis, Department of Civil Engineering, Queen's University at Kingston, Ontario, Canada.
- Rogers, C. D. (1988). Some observations on flexible pipe response to load. *Transportation Research Record*, No. 1191, 1–11.
- Tognon, A. R. M., Rowe, R. K. & Brachman, R. W. I. (1999). Evaluation of side wall friction for a buried pipe testing facility. *Geotextiles and Geomembranes*, **17**, No. 4, 193–212.
- White, D. J., Take, W. A. & Bolton, M. D. (2003). Soil deformation measurement using particle image velocimetry and photogrammetry. *Géotechnique*, **53**, No. 7, 619–631.

The Editor welcomes discussion on all papers published in Geosynthetics International. Please email your contribution to discussion@geosynthetics-international.com by 15 October 2008.